# Presence of π...π and C-H...π interactions in the new Schiff base 2-{(*E*)-[(3-*tert*-butyl-1-phenyl-1*H*-pyrazol-5-yl)imino]methyl}phenol: Experimental and DFT computational studies

**Rodolfo Moreno-Fuquen[a], Fernando Cuenú[b], John Eduard Torres[b], Gala De la Vega[a], Esperanza Galarza[a], Rodrigo Abonia[a], Alan R. Kennedy[c]**

[a]Departamento de Química, Universidad del Valle, Calle 13 Carrera 100. AA 25630, Cali-Colombia

[b]Laboratorio de Química Inorgánica y Catálisis, Programa de Química, Universidad del Quindío, Carrera 15, Calle 12 Norte, Armenia-Colombia

[c]Department of Pure & Applied Chemistry. University of Strathclyde, 295 Cathedral Street, Glasgow G1 1XL Scotland

*Corresponding author. Email: rodolfo.moreno@correounivalle.edu.co, Tel: +05723393248

## ABSTRACT

A combined theoretical and experimental study on the structure, infrared and UV-Vis data of 2-{(*E*)-[(3-*tert*-butyl-1-phenyl-1*H*-pyrazol-5-yl)imino]methyl}phenol (**3**), is presented. Theoretical geometry optimization and its IR spectrum were carried out using the Density Functional Theory (DFT), while for the theoretical UV-Vis spectrum, the Time-Dependent DFT (TD-DFT) method was used. The supramolecular analysis of the compound evidenced the presence of π ... π interactions between the phenol and pyrazole rings and the presence of C-H...π interactions between the methyl group and the phenyl rings which form chains of molecules parallel to the plane (100).

## Keywords

Schiff bases, Crystal structure, FT-IR and NMR spectroscopy, Electronic absorption spectra, DFT calculations.

## 1. Introduction

Fused pyrazoles and their derivatives exhibit a wide range of interesting biological properties such as analgesics, anti-inflammatory, antitubercular, antipyretic, antibacterial and anticancer agents.[1-5] Imines possess the general formula $R^1R^2C=NR^3$, they also are named as Schiff bases because they were firstly synthesized by Hugo Schiff in 1864, *via* a condensation reaction method between primary amines and aldehydes or ketones.[6,7] This family of compounds have widely been studied because of their interesting physicochemical properties related to their structures, this fact, have made them the object of many theoretical and experimental investigations.[8-9] The most important features of the Schiff bases or their metal complexes it can be counted: their catalytic[10-12] and biological activities,[13-15] their application as metal ion sensors,[16-18] molecular disruptor[19-22] and also as anti-cancer agents,[23-24] among others.

On the other hand, structural X-ray diffraction analysis allows the observation of possible specific properties in different molecular systems, from molecular orderings in the solid state. Some crystal systems can define their packing without the presence of hydrogen bonds or other strong intermolecular interactions. A great number of researchers have done their best in the search of a face-to-face π…π stacking array in the solid-state packing of organic semiconductors to improve the electrical characteristics of these compounds using excellent intermolecular π…π interactions.[25-26] In this paper, the experimental and calculated spectroscopic properties of the title compound prepared by the reaction of 3-*tert*-butyl-1-phenyl-1*H*-pyrazol-5-amine with salicylaldehyde, are compared and their possible π…π and C-H... π interactions are studied.

## 2. Experimental

### 2.1 Materials and Methods

General information

Reaction was monitored by thin layer chromatography (TLC), using Silica gel aluminum plates (Merck 60 $F_{254}$). Melting point was determined on a Büchi melting point B-450 apparatus. IR spectrum was recorded on a Perkin-Elmer FT spectrophotometer series 2000 using KBr disks. NMR spectra were recorded on a Bruker Avance 400 spectrometer operating at 400.13 MHz for $^1$H and 100.61 MHz for $^{13}$C, using DMSO-$d_6$ as solvent and tetramethylsilane as an internal standard. Chemical shifts ($\delta$) are in ppm, coupling constants ($J$) are in Hertz (Hz) and the classical abbreviations are used to describe the signal multiplicities. The mass spectrum was obtained on a SHIMADZU-GCMS 2010-DI-2010 spectrometer equipped with a direct inlet probe operating at 70 eV. High resolution mass spectrum (HRMS) was recorded on an Agilent Technologies Q-TOF 6520 spectrometer *via* an electrospray ionization (ESI). Microanalyses was performed on an Agilent elemental analyzer and the values are within 0.4% of the theoretical. The UV–Vis absorption spectrum of compound **3** was obtained in acetonitrile solution at room temperature in the range of 200–600 nm using an UV-Vis 160A SHIMADZU Spectrophotometer. Chemicals and solvents were purchased from Sigma-Aldrich and Across, and were used without further purification.

## 2.2 Synthesis

A sample of the 3-*tert*-butyl-1-phenyl-1*H*-pyrazol-5-amine (**1**) was prepared as described in the literature.[27] To a solution of concentrated hydrochloric acid (3.8 mL) in water (33 mL), phenylhydrazine (2.1220 g, 19.62 mmol) and 4,4-dimethyl-3-oxopentanenitrile (1.8502 g, 14.78 mmol) were added. The mixture was heated at 70 °C for 1 h, then concentrated hydrochloric acid (3.8 mL) was added and the mixture was heated additionally for 1 h. After cooling, crushed ice was added and the mixture was neutralized with concentrated ammonium hydroxide. The resulting solid was filtered under reduced pressure, washed with cold water (3 x 5 mL) and dried at ambient temperature affording the compound **1** as a pale yellow solid.

Synthesis of compound **3** (see Scheme 1). A mixture of 3-*tert*-butyl-1-phenyl-1*H*-pyrazol-5-amine **1** (0.231 g, 1.075 mmol), salicylaldehyde **2** (0.134 g, 1.093 mmol) and acetic acid (5 drops) was stirred for ten minutes. Until the reaction was complete (TLC control), the yellow solid formed was washed with water (5 x 20 mL) and dried under vacuum to afford compound **3** (0.325 g, 95% yield). Single crystals suitable for X-ray diffraction were grown from $CH_2Cl_2$ by slow evaporation at room temperature.

**Insert Scheme 1**

Anal. Calc. for $C_{20}H_{21}N_3O$: C% 75.21; H% 6.63; N% 13.16. Found: C% 75.31; H% 6.59; N% 13.12. M.p. 401.8 K. (MS, 70 eV) *m/z* (%) 319 ($M^+$, 100), 302 ($M^+$- 17, 14.58), 304 ($M^+$ - 15, 77.76), 57 (6.61). IR ( KBr, $cm^{-1}$) $\nu$ Ph-H 3060.63, $\nu_{as}$ –$CH_3$ 2958.41, $\nu_s$ –$CH_3$ 2863.91, $\nu$ –C=N 1604.56. $^1$H NMR (400 MHz) (DMSO-$d_6$, $\delta$ in ppm): 1.33 (bs, 9H, H-[12, 13, 14]), 6.69 (bs, 1H, H-9), 6.93 (d, 1H, $^3J$ = 8.4 Hz, H-3); 6.99 (t, 1H, $^3J$ = 7.4 Hz, H-18), 7.41 (m, 1H, $^3J$ = 7.6 Hz, H-4); 7.42 (m, 1H, H-5); 7.54 (t, 2H, $^3J$ = 7.4 Hz, H-17, 19); 7.61 (d, 2H, $^3J$ = 7.8 Hz, H-16, 20); 7.67 (d, 1H, $^3J$ = 7.6 Hz, H-6); 9.12 (bs, 1H, H-7); 11.76 (s, 1H, OH); NMR $^{13}$C (400 MHz) (DMSO-$d_6$, $\delta$ in ppm): 30.7 (C-12), 32.7 (C-11), 91.5 (C-9), 117.1 (C-3), 119.9 (C-18), 120.1 (C-1), 124.5 (C-20), 127.4 (C-4), 129.3 (C-19), 132.4 (C-6), 134.3 (C-5), 139.3 (C-15), 148.7 (C-8), 160.11 (C-2), 162.0 (C-10), 163.1 (C-7), UV-Vis in MeCN, $\lambda$máx nm, (log $\boldsymbol{\varepsilon}$), $\lambda_1$ 197 (5.36), $\lambda_2$ 219 (4.79), $\lambda_3$ 233 (4.79), $\lambda_4$ 276 (4.42), $\lambda_5$ 308 (4.53), $\lambda_6$ 324 (4.54), $\lambda_7$ 357 (4.59), $\lambda_8$ 381 (4.37).

Note: The assignment of the signals in $H^1$NMR and $^{13}C$ NMR was performed in relation to figure 1(a).

### 3. Computational study for compound 3

All the theoretical calculations were determined in gas phase and in the approximation of the isolated molecule, using GaussView05 program[28] and Gaussian09[29] program package. The molecular optimization, harmonic vibrational frequency, NMR and energy studies were calculated by *ab initio* computational methods Hartree-Fock (HF) and Density Functional Theory (DFT), using hybrid density functional B3LYP with the 6–311++G (d,p) basis, without any obstacle for the geometry. Theoretical vibrational spectra of compound **3** were interpreted by means of potential energy distributions (PEDs) using VEDA 4 program.[30] Vibrational frequencies and bond lengths found at the DFT methods, yield better results when compared the experimental values with those obtained by Hartree-Fock methods.

### 4. Results and discussion

### 4.1 Single crystal X-ray diffraction study

**4.1.1 Crystal Data:** $C_{12}H_{21}N_3O$ (M = 319.40 g/mol): monoclinic, space group P $2_1/c$ (No. 14), a = 11.4508(8) Å, b = 14.0285(8) Å, c = 11.7440(8) Å, α = 90.0, β = 115.667(8), γ = 90.0, V = 1700.4(2) $Å^3$ , Z = 4, T = 123(2) K, μ($MoK_\alpha$) = 0.079 $mm^{-1}$, $D_{cal}$= 1.248 $Mg/m^3$, 8142 reflections measured ($3.483^o \leq \Theta \leq 26.999^o$), index range: $-14 \leq h \leq 10$, $-15 \leq k \leq 17$, $-14 \leq l \leq 14$, 3700 unique ($R_{int}$ = 0.0288, $R_{sigma}$= 0.0483) which were used in all calculations. Refinement method: Full-matrix least-squares on $F^2$. The final R1 was 0.0474 ($I > 2\sigma(I)$) and wR2 was 0.1177 (all data). Largest diff. peak and hole 0.238 and -0.222 e.$Å^{-3}$

**4.1.2 Data Collection and Refinement Details:** Diffraction data were collected on an Oxford Diffraction Xcalibur E diffractometer using CrysAlis PRO,[31] using graphite monochromated $MoK_\alpha$ radiation (0.71073 Å). The corrected data were solved by direct methods with SHELXS-2014[32] and refined by full-matrix methods on $F^2$ with SHELXL-2014.[33] All H-atoms, were positioned at geometrically idealized positions, C—H= 0.9500 Å, C—H= 0.9800 Å for methyl, and they were refined using a riding model approximation with Uiso(H) = 1.2 and 1.5 $U_{eq}$(parent atom). H1H atom was found from the Fourier maps and its coordinates were refined freely. Correctness of the model was confirmed by low residual peaks (0.238) and holes (-0.222 e.$Å^3$) in the final difference map.

### 4.2 Molecular Geometry

The optimized structure parameters of compound **3** calculated by HF and DFT methods listed in Table 1 are in accordance with atom numbering given in Figure 1.

The central segment, C1–C7–N1–C8 (r.m.s. deviation = 0.0159 Å), is rotated by 4.58 (15)°, 4.20 (18)° and 53.76 (6)° to the phenol (A), pyrazole (B) and phenyl (C) rings, respectively. These values show an approximate planarity between phenolic (A) and pyrazole (B) rings respectively, thus obtaining a higher conjugation in that region of the molecule. The properties of planarity and conjugation are broken when trying to include the third ring of the molecule.

**Insert Table 1**

**Insert Figure 1(a)** **Insert Figure 1(b)**

### 4.3 Supramolecular behavior

At supramolecular level, classical hydrogen bond interactions and other common C-H…X (X= O, N) hydrogen bond contacts are not detected in compound **3**, whereas π… π and C-H…π interactions are observed. In the literature a similar compound, the 3-*t*Butyl-5-((4-methoxybenzylidene)amino)-1-phenylpyrazole (CSD refcode VAGYOS)[34], with the presence of C-H…π interaction, is reported. The central segment C1-C7-N1-C8 in compound **3**, presents approximate planarity with the phenol (A) and pyrazole (B) rings but does not observe planarity with the phenyl (A) ring. This planarity, possibly induces the phenol and pyrazole rings to orient themselves face to face in crystalline growth. This approach allows π…π interactions to become more effective. Recent studies have considered π…π non-binding interactions as responsible for crystal growth.[35-36] Analysis of the crystalline growth of compound **3** shows that, effectively, it is developed into face to face π… π and C-H… π stacking.

The facing phenol (A) and pyrazole (B) rings observe a distance of 3.771 Å, between their centroid positions $C_{g1}\ldots C_{g2}^{i}$ (i= 2-x,1-y,-z) and they are interwoven with other molecules by C-H… π interactions. The latter interaction is carried out between one of the carbons (C13) of the *tert*-butyl group and the phenol (A) ring of the neighboring molecule, showing a C-H... $C_{g3}^{ii}$ (ii = x,1/2-y,1/2-z) with a distance of 3.535 Å. These interactions are shown running parallel to (100)

(see Fig. 2). The overlapping of the rings is accentuated by the highly $\pi$ delocalized resonant contributor **"3"** in which the phenolic moiety (A) acquires a partial positive charge while the pyrazole moiety (B) acquire the negative one, as shown in Scheme 2.

**Insert Figure 2 (a)** **Insert Figure 2 (b)**

**Insert Scheme 2**

Both (A) and (B) moieties interacts favorably in a head (+)-to-tail (-) fashion in the supramolecular structure, acquiring a good tendency to form face-to-face $\pi\ldots\pi$ interactions,[37] as shown in Fig. 2. These latter interactions were visualized using the Hirshfeld surface, Fig. 3(a). On the surface can be observed red spots that show the regions of interaction with other molecules, specifically between the phenol (A) and pyrazole (B) rings. The absence of other stronger interactions, such as hydrogen bonds, can be seen in Fig. 3(b) where the interaction matrix does not show the characteristic claws or peaks for these kind of bonds.

**Insert Figure 3(a)** **Insert Figure 3(b)**

The most important contributions of intermolecular contacts to the Hirshfeld surfaces were, H...H (61.3%), C…H (17.8%), N…H (6.1%), C…C(6.3%) (Fig. 3(b)).

### 4.4 Vibrational analysis

The application of the Fourier transform in certain techniques of analysis, enabled the IR spectroscopy to emerge and be placed at the present time as one of the most used analysis tools for the characterization of materials. The FT-IR spectrum has been recorded and its vibrational assignment is presented for compound **3** for the first time. In this section we will discuss the IR characteristic bands and their assignments based on the comparison between the solid IR experimental state spectrum and the results obtained through the use of the DFT/B3LYP/6-311G++(d,p) model. The experimental and calculated spectra are shown in Fig. 4. The scale factor used with the theoretical values was 0.9619.[38] For the assignment of the

frequencies it was used VEDA 4,[30] with its corresponding PED% value. According to VEDA 4, theoretical spectrum have good agreement with the experimental FT-IR one.

**Insert Figure 4(a)**

**Insert Figure 4(b)**

### 4.4.1 Hydroxyl group vibrations

The hydroxyl O-H stretching (vOH), is generally a strong and broad band, that can be observed in a region around 3500 $cm^{-1}$.[39] Our experimental results show a vOH band at 3120 $cm^{-1}$ and it is similar to values shown by other authors.[40-41] Calculated value is obtained at 3195 $cm^{-1}$. The difference between these values emerges as a result of which the calculations do not consider the interaction generated by the iminic nitrogen over the phenolic hydrogen generating a relative strong intramolecular hydrogen bond. The frequency due to O-H in-plane bending vibration, in general, is located in the region 1150–1250 $cm^{-1}$. The experimental spectrum shows a medium-strong FT-IR band at 1121 $cm^{-1}$ and the calculated value is 1128 $cm^{-1}$. The frequency due to O-H out of-plane bending vibration is located in general in the region 650-770 $cm^{-1}$. Our results show a band at 775 $cm^{-1}$ and its calculated value at 781 $cm^{-1}$.

### 4.4.2 C-H vibrations

The aromatic C-H stretching vibrations are in general observed in the region 3000–3100 $cm^{-1}$. In compound **3**, a C-H stretching vibration of the rings (A, B and C) is observed at 3059 $cm^{-1}$. This is in agreement with experimental assignment 3040–3089 $cm^{-1}$.[42] Three calculated frequencies for C-H symmetric mode, C-H asymmetric mode in phenol (A) ring and C-H asymmetric mode in phenyl (C) ring at 3071 $cm^{-1}$, 3065 $cm^{-1}$ and 3064 $cm^{-1}$ respectively, were assigned. The 2958 $cm^{-1}$ band is assigned to $CH_3$ asymmetric mode, while the weak band at 2862 $cm^{-1}$ correspond to the $CH_3$ symmetric mode. Calculated stretching bands at 2968 and 2907 $cm^{-1}$ were assigned for these vibrations, respectively. These values are in a good agreement with other reported studies.[43]

### 4.4.3 C=N vibrations

The stretching vibration band C=N is observed in the region 1500-1620 $cm^{-1}$.[44-45] A strong band observed at 1570 $cm^{-1}$ in the FTIR spectrum is assigned to C=N stretching vibration mode. Calculated stretching band at 1582 $cm^{-1}$, is assigned to this vibration.

### 4.4.4 C-O vibrations

The stretching vibration band C-O is observed in the region 970-1250 $cm^{-1}$.[46] A strong band observed at 1281 $cm^{-1}$ in the FTIR spectrum was assigned to C-O stretching vibration mode. Calculated stretching band at 1262 $cm^{-1}$, was assigned to this vibration. See Fig. 5(a) and 5(b).

**Insert Figure 5(a)** **Insert Figure 5(b)**

**4.5 UV-Vis**

The most important orbitals in a molecule are its frontier molecular orbitals that determine how the molecule interacts with other species. A molecule with a small HOMO-LUMO energy gap is more polarizable and is generally related to a high chemical reactivity or a low kinetic stability.[47] HOMO is the orbital that acts as an electron donor and LUMO is the orbital that acts as an electron acceptor. The electronic transition energies were calculated using the Time Dependent Density Function Theory (TD-DFT),[48-50] with the 6-311++G(d,p) basis set optimized structure in acetonitrile solvent.

The measured values of absorption wavelengths $\lambda_{max}$ in compound **3**, are at 235 and 363 nm, and they can be assigned to $\pi \rightarrow \pi^*$ transition.[51] UV-Vis spectrum, and are in good agreement with the experimental data. The calculated UV-Vis absorption bands were obtained at 236.88 nm, 238.97 nm and 365.04 nm. From Fig. 6 (a) and 6 (b) it can be seen that the HOMO is uniformly distributed in the central segment and over the phenol (A) and pyrazole (B) rings. From Figure 6a and 6b, it can be seen that HOMO is uniformly distributed on the central segment and on the phenol (A) and pyrazole (B) rings and that this distribution is partial on the phenyl (C) ring and on the *tert*-butyl group, whereas LUMO (Fig. 6a) is distributed similarly to HOMO except for its presence on the *tert*-butyl group and partially showing its distribution on the pyrazole (B) ring. The LUMO+3 is distributed over the phenol (A) and phenyl (C) rings and partially over the central segment (Fig.6 b). In the HOMO-1 a uniform distribution is observed on the pyrazole (B) and phenyl (C) rings. This orbital also shows a partial distribution on the phenol (A) ring and a null distribution on the central segment. LUMO+1 shows a partial distribution over the central segment Fig. 6 c and a substantial increase over the phenyl (C) ring as shown in 6(c).

**Insert Figure 6**

## 5. Conclusions

Single crystal X-ray crystallography clearly showed the structural conformation of compound **3**. The planar behavior of the phenol (A) and pyrazole (B) aromatic rings with the central segment C1-C7-N1-C8 became evident. The supramolecular analysis evidenced the presence of π ... π interactions between the phenol (A) and pyrazole (B) rings, which in turn are related by inversion centers. Additionally, the presence of C-H...π interactions between the methyl group and the phenyl (C) ring, which acts as junction to form chains of molecules parallel to the plane (100). These interactions were evidenced using Hirshfeld's surface theory, clearly showing the interactions between the phenol (A) and pyrazole (B) rings. The absence of other interactions, different from those analyzed, was evidenced in the fingerprint. The values obtained in the HOMO-LUMO gaps of the present study show a good stability of the molecule as well as relative chemical reactivity. Other spectroscopic techniques ($^{1}$H and $^{13}$C NMR) were used to confirm the results of the present study. Calculations performed by DFT using hybrid methods, type B3LYP, have shown their goodness in establishing excellent approximations with the experimental parameters. The above was demonstrated by the calculations performed on within this work in relation to IR or-and UV-Vis spectroscopy.

## 6. Acknowledgement

The authors thank the Universidad del Valle and Universidad del Quindío for partial financial support (Project 789).

## Supporting information

(CCDC 1551653 contains the supplementary crystallographic data for this paper. These data can be obtained free of charge via http://www.ccdc.cam.ac.uk/conts/retrieving.html (or from the CCDC, 12 Union Road, Cambridge CB2 1EZ, UK; Fax: +44 1223 336033; E-mail: deposit@ccdc.cam.ac.uk).

## 7. References

[1] N. Nayak, J. Ramprasad, U. Dalimba. J. Flourine Chem. 183 (2016) 59–68, https://doi.org/10.1016/j.jfluchem.2016.01.011

[2] R.D. Kamble, R.J. Meshram, S.V. Hese, R.A. More, S.S. Kamble, R.N. Gacche, B.S. Dawane. Comput. Biol. Chem. 61 (2016) 86–96, http://dx.doi.org/doi:10.1016/j.compbiolchem.2016.01.007

[3] K. Karrouchia, L. Chemlal, J. Taoufik, Y. Cherrah, S. Radi, M.A. Faouzi, M. Ansar. Ann. Pharm. Fr. 74 (2016) 431-438, https://www.ncbi.nlm.nih.gov/pubmed/27107461

[4] F.A. Ragab, N.M.A. Gawad, H.H. Georgey, M.F. Said. Eur. J. Med. Chem. 63 (2013) 645–654, https://doi.org/10.1016/j.ejmech.2013.03.005

[5] A.M. Saleh, M.O. Taha, M.A. Aziz, M.A. Al-Qudah, R.F. AbuTayeh, S.A. Rizvi. Cancer Lett. 375 (2016) 199–208, https://doi.org/10.1016/j.canlet.2016.02.028

[6] H. Schiff. Justus Liebigs Ann. Chem. 131 (1864) 118-119, http://onlinelibrary.wiley.com/doi/10.1002/jlac.18641310113/abstract

[7] V.T. Kasumov, F. Koksal. Spectrochim. Acta A: Mol. Biomol. Spectrosc. 61 (2005) 225-232, https://doi.org/10.1016/j.saa.2004.03.037

[8] A.Ö. Yildirim, Ç.A. Kastas, M. Gülsu. J. Mol. Struct. 1103 (2016) 311-318, https://doi.org/10.1016/j.molstruc.2015.09.029

[9] N. Benarous, A. Cherouana, E. Aubert, P. Durand, S. Dahaoui. J. Mol. Struct. 1105 (2016) 186-193, https://doi.org/10.1016/j.molstruc.2015.10.037

[10] O.V. Nesterova, E.N. Chygorin, V.N. Kokozay, V.V. Bon, I.V. Omelchenko, O.V. Shishkin, J. Titis, R. Boca, A.J.L. Pombeiro, A. Ozarowski. Dalton Trans. 42 (2013) 16909–16919, http://pubs.rsc.org/-/content/articlelanding/2013/dt/c3dt51800k#!divAbstract

[11] M. Amini, M. Khaksar, D.M. Boghaei, M. Bagherzadeh, A. Ellern, L.K. Woo. J. Coord. Chem. 67 (2014) 2435–2444, http://dx.doi.org/10.1080/00958972.2014.939076

[12] W. Ren, L. Chen, N. Zhao, Q. Wang, G. Hou, G. Zi. J. Organomet. Chem. 758 (2014) 65–72, https://doi.org/10.1016/j.jorganchem.2014.02.005

[13] M.D. Peterson, R.J. Holbrook, T.J. Meade, E.A. Weiss. J. Am. Chem. Soc. 135 (2013) 13162–13167, http://pubs.acs.org/doi/abs/10.1021/ja4065393

[14] N.E. Kassan, H.A. Saadeh, W.H. Talib, A.M. Mahasneh, H. Kaur, K. Goyal, R. Sehgal, M.S. Mubarak. Med. Chem. Res. 23 (2014) 4872–4882, https://link.springer.com/article/10.1007/s00044-014-1055-4

[15] N.A. Mazlan, T.B.S.A. Ravoof, E.R.T. Tiekink, M.I.M. Tahir, A. Veerakumarasivam, K.A. Crouse. Trans. Metal Chem. 39 (2014) 633–639, https://link.springer.com/article/10.1007/s11243-014-9842-9

[16] S. Kumari, G.S. Chauhan. ACS Appl. Mater. Interf. 6 (2014) 5908–5917, http://pubs.acs.org/doi/abs/10.1021/am500820n

[17] Y. Zhou, Z.X. Li, S.Q. Zang, Y.Y. Zhu, H.Y. Zhang, H.W. Hou, T.C.W. Mak. Org. Lett. 14 (2012) 1214–1217, http://pubs.acs.org/doi/abs/10.1021/ol2034417

[18] R. Azadbakht, H. Keypour, H.A. Rudbari, A.H.M. Zaheri, S. Menati. J. Lumin. 132 (2012) 1860–1866, http://dx.doi.org/10.1016/j.jlumin.2012.02.035

[19] R. Azadbakht, J. Khanabadi. Spectrochim. Acta A: Mol. Biomol. Spectrosc. 124 (2014) 249–255, https://doi.org/10.1016/j.saa.2014.01.015

[20] C. Gahl, D. Brete, F. Leyssner, M. Koch, E.R. McNellis, J. Mielke, R. Carley, L. Grill, K. Reuter, P. Tegeder, M. Weinelt. J. Am. Chem. Soc. 135 (2013) 4273-4281, http://pubs.acs.org/doi/abs/10.1021/ja309330e

[21] M.E. Belowich, J.F. Stoddart. Chem. Soc. Rev. 41 (2012) 2003–2024, https://www.ncbi.nlm.nih.gov/pubmed/22310886

[[22] J. Mielke, F. Leyssner, M. Koch, S. Meyer, Y. Luo, S. Selvanathan, R. Haag, P. Tegeder, L. Grill. ACSNano 5 (2011) 2090–2097, http://pubs.acs.org/doi/abs/10.1021/nn103297e

[23] A. Chakraborty, P. Kumar, K. Ghosh, P. Roy. Eur. J. Pharmacol. 647 (2010) 1–12, https://www.ncbi.nlm.nih.gov/pubmed/20797395

[24] S. Sathiyaraj, K. Sampath, R.J. Butcher, R. Pallepogu, C. Jayabalakrishnan. Eur. J. Med. Chem. 64 (2013) 81–89, https://doi.org/10.1016/j.ejmech.2013.03.047

[25] X.C. Li, H. Sirringhaus, F. Garnier, A.B. Holmes, S.C. Moratti, N. Feeder, W. Clegg, S.J. Teat, S., R.H. Friend. J. Am. Chem. Soc. 120 (1998) 2206-2207, http://pubs.acs.org/doi/abs/10.1021/ja9735968

[26] J.G. Laquindanum, H.E. Katz, A.J. Lovinger, A. Dodabalapur. Adv. Mater. 9 (1997) 36-39, http://onlinelibrary.wiley.com/doi/10.1002/adma.19970090106/abstract

[27] (a) J. Quiroga, J. Portilla, R. Abonia, B. Insuasty, M. Nogueras, J. Cobo. Tetrahedron Lett. 49 (2008) 6254–6256, https://doi.org/10.1016/j.tetlet.2008.08.044. (b) S. Hernández-Ortega, F. Cuenú-Cabezas, R. Abonía-González, A. Cabrera-Ortiz. Acta Cryst. E68 (2012) o3171, http://journals.iucr.org/e/issues/2012/11/00/bt6847/bt6847.pdf

[28] R. Dennington, T. Keith, J. Millam. GaussView. Version 5. Shawnee Mission KS: Semichem Inc; 2009.

[29] M.J. Frisch, G.W. Trucks, H.B. Schlegel, G.E. Scuseria, M.A. Robb, J.R. Cheeseman, G. Scalmani, V. Barone, B. Mennucci, G.A. Petersson, H. Nakatsuji, M. Caricato, X. Li, H.P. Hratchian, A.F. Izmaylov, J. Bloino, G. Zheng, J.L. Sonnenberg, M. Hada, M. Ehara, K. Toyota, R. Fukuda, J. Hasegawa, M. Ishida, T. Nakajima, Y. Honda, O. Kitao, H. Nakai, T. Vreven, J.A. Montgomery, Jr., J.E. Peralta, F. Ogliaro, M. Bearpark, J.J. Heyd, E. Brothers, K.N. Kudin, V.N. Staroverov, R. Kobayashi, J. Normand, K. Raghavachari, A. Rendell, J.C. Burant, S.S. Iyengar, J. Tomasi, M. Cossi, N. Rega, J.M. Millam, M. Klene, J.E. Knox, J.B. Cross, V. Bakken, C. Adamo, J. Jaramillo, R. Gomperts, R.E. Stratmann, O. Yazyev, A.J. Austin, R. Cammi, C. Pomelli, J.W. Ochterski, R.L. Martin, K. Morokuma, V.G. Zakrzewski, G.A. Voth, P. Salvador, J.J. Dannenberg, S. Dapprich, A.D. Daniels, Ö. Farkas, J.B. Foresman, J.V. Ortiz, J. Cioslowski, D.J. Fox, Gaussian 09, Revision D.01, Gaussian, Inc., Wallingford CT, 2013.

[30] M.H. Jamróz. Spectrochim. Acta A: Mol. Biomol. Spectrosc. 114 (2013) 220-230, http://dx.doi.org/10.1016/j.saa.2013.05.096

[31] Oxford Diffraction (2010). CrysAlis PRO. Oxford Diffraction Ltd, Yarnton, England. https://www.rigaku.com/en/products/smc/crysalis

[32] G.M. Sheldrick. Acta Cryst. A64 (2008) 112–122, https://www.ncbi.nlm.nih.gov/pmc/articles/PMC4294323/

[33] G.M. Sheldrick. Acta Cryst. C71 (2015) 3–8, https://www.ncbi.nlm.nih.gov/pmc/articles/PMC4294323/

[34] J.N. Low, J. Cobo, M. Nogueras, A. Sánchez, E. Rengifo, R. Abonia. Acta Cryst. E59 (2003) o250-o252, http://scripts.iucr.org/cgi-bin/paper?S1600536803001909

[35] J.E. Anthony, J.S. Brooks, D.L. Eaton, S.R. Parkin. J. Am. Chem. Soc. 123 (2001) 9482-9483, http://pubs.acs.org/doi/abs/10.1021/ja0162459

[36] K. Kobayashi, H. Masu, A. Shuto, K. Yamaguchi. Chem. Mater. 17 (2005) 6666-6673, http://pubs.acs.org/doi/abs/10.1021/cm051874t

[37] T.-D. Kim, J.-W. Kang, J. Luo, H.-S. Jang, J.-W. Ka, N. Tucker, J.B. Benedict, L.R. Dalton, T. Gray, R.M. Overney, D.H. Park, W.N. Herman, A.K.-Y. Jen. J. Am. Chem. Soc. 129 (2007) 488-489, http://pubs.acs.org/doi/abs/10.1021/ja067970s

[38] M.P. Andersson, P. Uvdal. J. Phys. Chem. A. 109 (2005) 2937–2941, http://pubs.acs.org/doi/abs/10.1021/jp045733a

[39] B. Smith. Infrared Spectral Interpretation. A Systematic Approach. CRC, Washington DC, 1999.

[40] V. Krishnakumar, V. Balachandran. Spectrochim. Acta A: Mol. Biomol. Spectrosc. 61 (2005) 2510–2525, https://doi.org/10.1016/j.saa.2004.08.026

[41] N. Sundaraganesan, B. Anand, C. Meganathan, B.D. Joshua. Spectrochim. Acta A: Mol. Biomol. Spectrosc. 68 (2007) 561–566, https://doi.org/10.1016/j.saa.2006.12.028

[42] M. Silverstein, G.C. Basseler, C. Morill. Spectrometric Identification of Organic Compounds. Wiley, New York, 1981.

[43] R.B. Viana, A.B.F. da Silva, A.S. Pimentel. Int. J. Mol. Sci. 13 (2012) 7980–7993, http://www.mdpi.com/1422-0067/13/7/7980/notes

[44] G. Zerbi, C. Alberti. Spectrochim. Acta 18 (1962) 407-423, https://doi.org/10.1016/S0371-1951(62)80149-0

[45] S. Gunasekaran, S. Seshadri, S. Muthu. Indian J. Pure Appl. Phys. 44 (2006) 581-586, http://www.niscair.res.in/ScienceCommunication/ResearchJournals/rejour/ijpap/ijpap2k6/ijpap_aug06.asp#a581

[46]https://www2.chemistry.msu.edu/faculty/reusch/virttxtjml/Spectrpy/InfraRed/infrared.htm

[47] I. Fleming. Frontier Orbitals and Organic Chemical Reactions. John Wiley and Sons, New York, 1976.

[48] M.E. Casida, C. Jamorski, K.C. Casida, D.R. Salahub. J. Chem. Phys. 108 (1998) 4439-4449,

http://aip.scitation.org/doi/abs/10.1063/1.475855

[49] L.M.L. Daku, J. Linares, M.-L, Boillot. PhysChemChemPhys. 12 (2010) 6107–6123, http://www.unige.ch/sciences/chifi/publis/refs_pdf/ref01039.pdf

[50] E. Runge, E.K.U. Gross. Phys. Rev. Lett. 52 (1984) 997-1000,

https://journals.aps.org/prl/abstract/10.1103/PhysRevLett.52.997

[51] H. Gökce, N. Öztürk, Ü. Ceylan, Y.B. Alpaslan, G. Alpaslan. Spectrochim. Acta A: Mol. Biomol. Spectrosc. 163 (2016) 170–180,
http://www.sciencedirect.com/science/article/pii/S1386142516301573

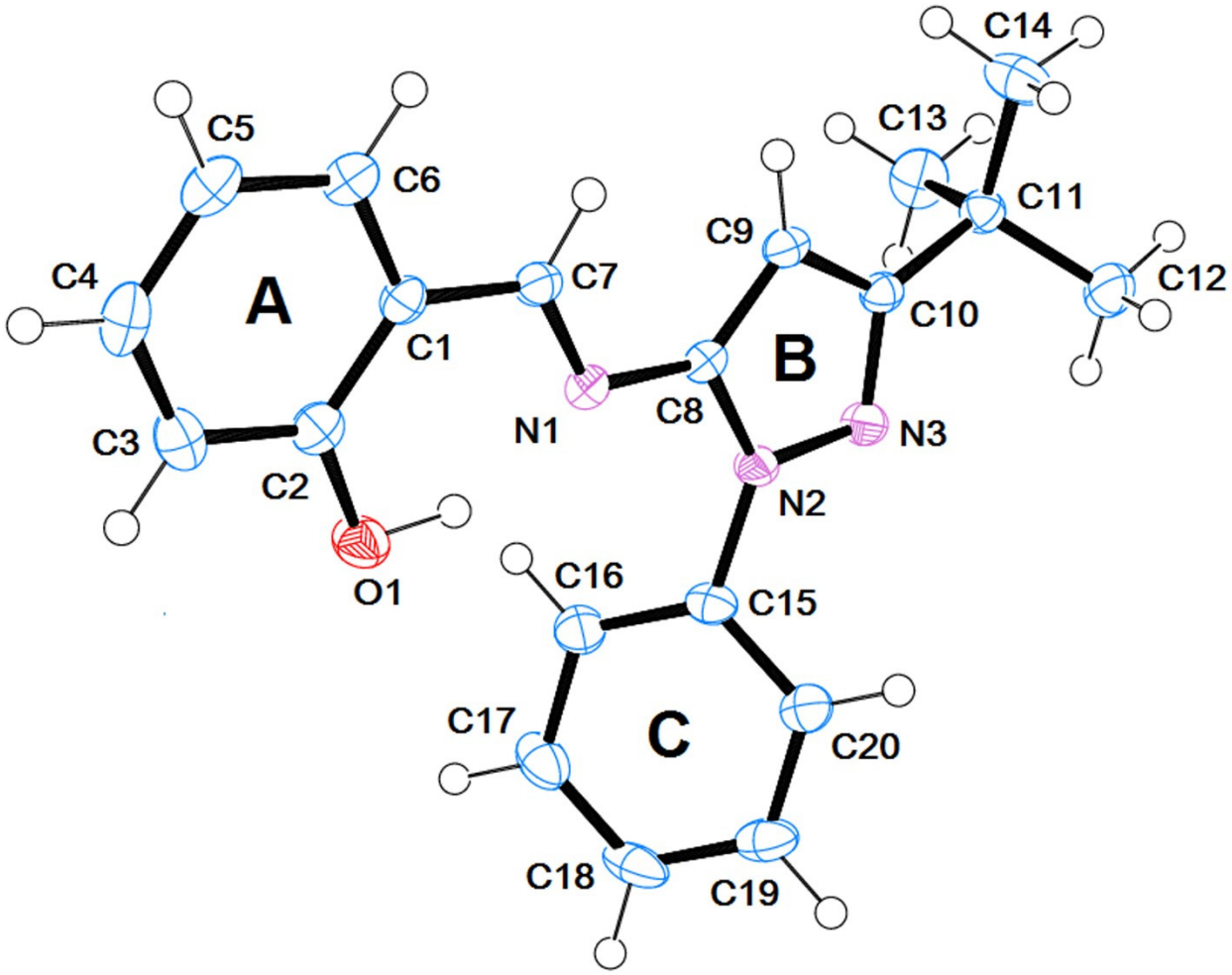
C14
C13
C5
C6
C11
C9
C4
A
C7
C12
C10
C1
B
N1
C8
C3
N3
C2
N2
O1
C16
C15
C17
C
C20
C18
C19

(a)

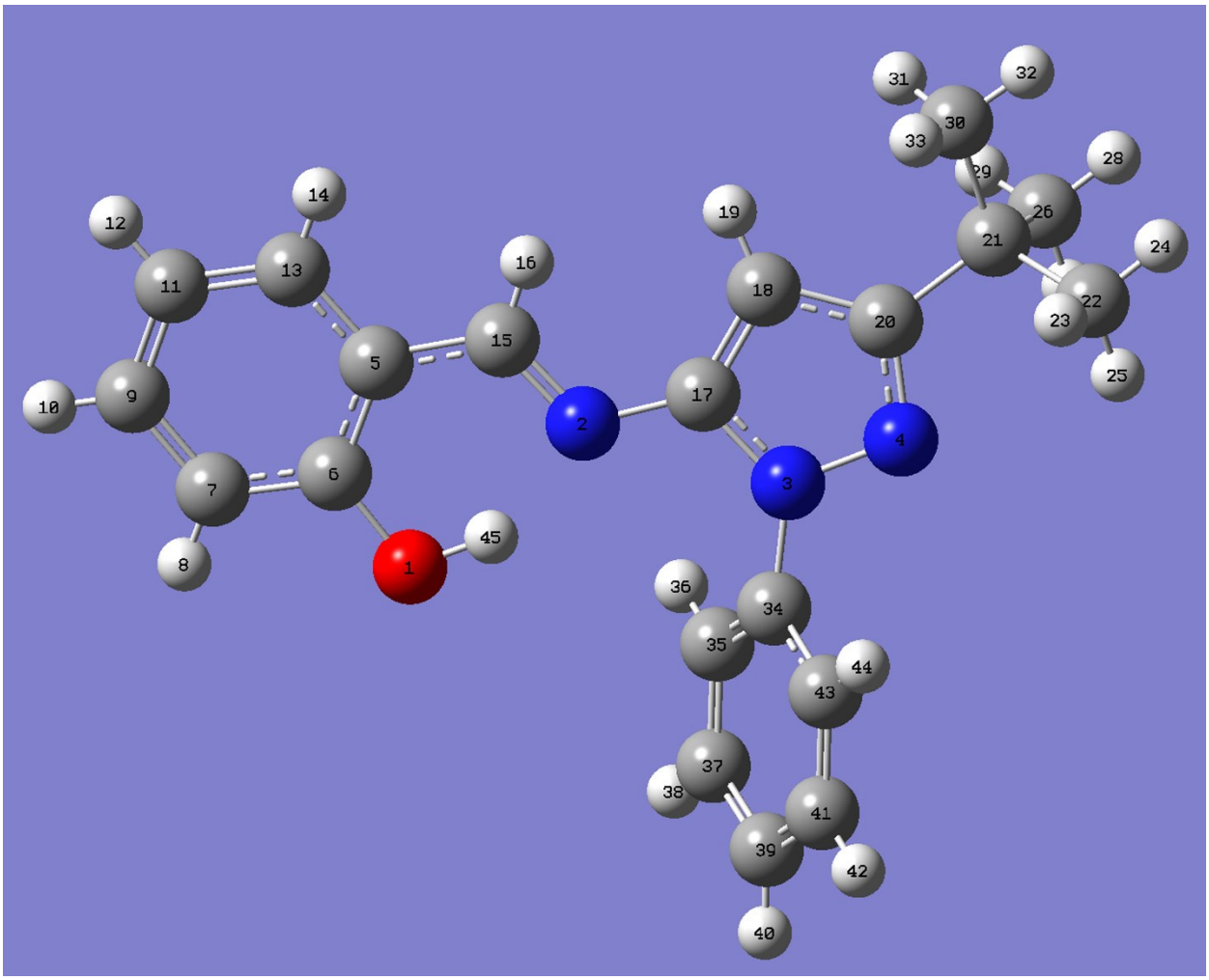


**(b)**

**Figure 1.** (a) Molecular structure of compound **3** obtained by X-ray diffraction, with thermal ellipsoids shown at the 50% probability level. (b) Calculated geometric parameters for compound **3** by using the DFT/B3LYP, 6–311++G (d,p) basis set.

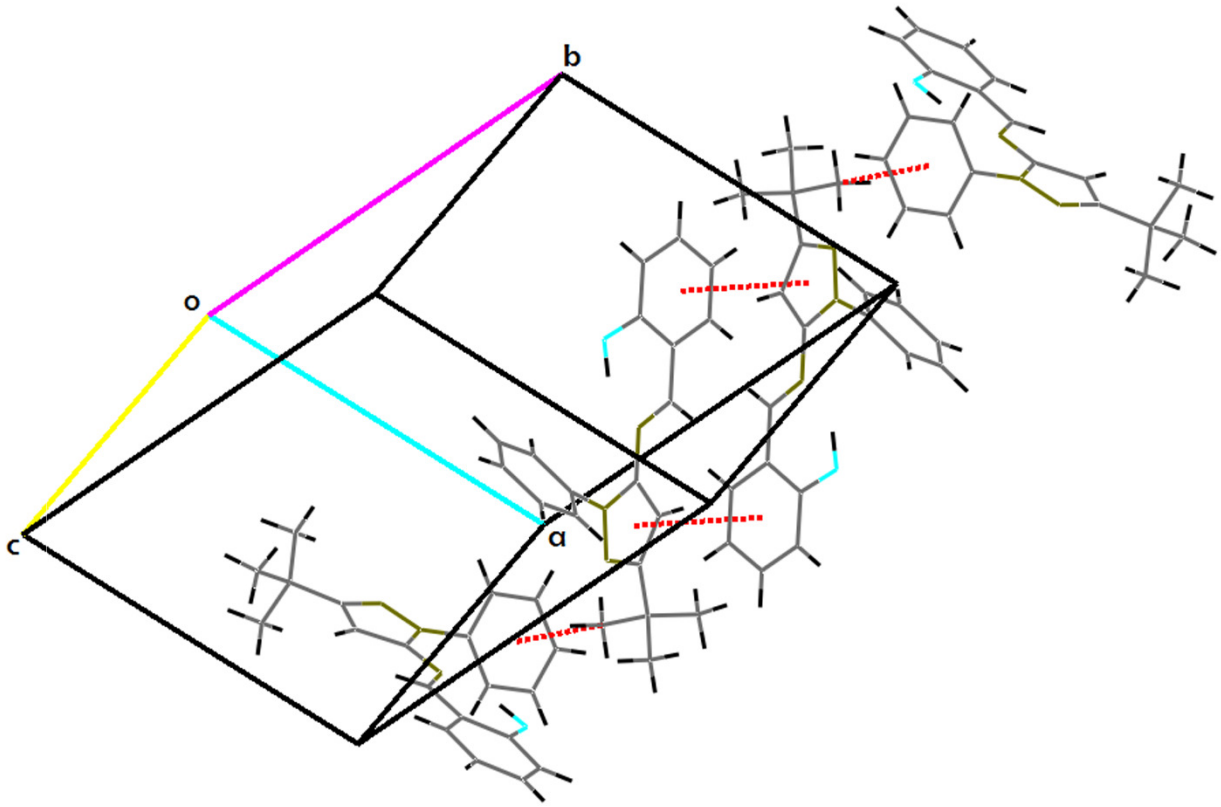


(a)

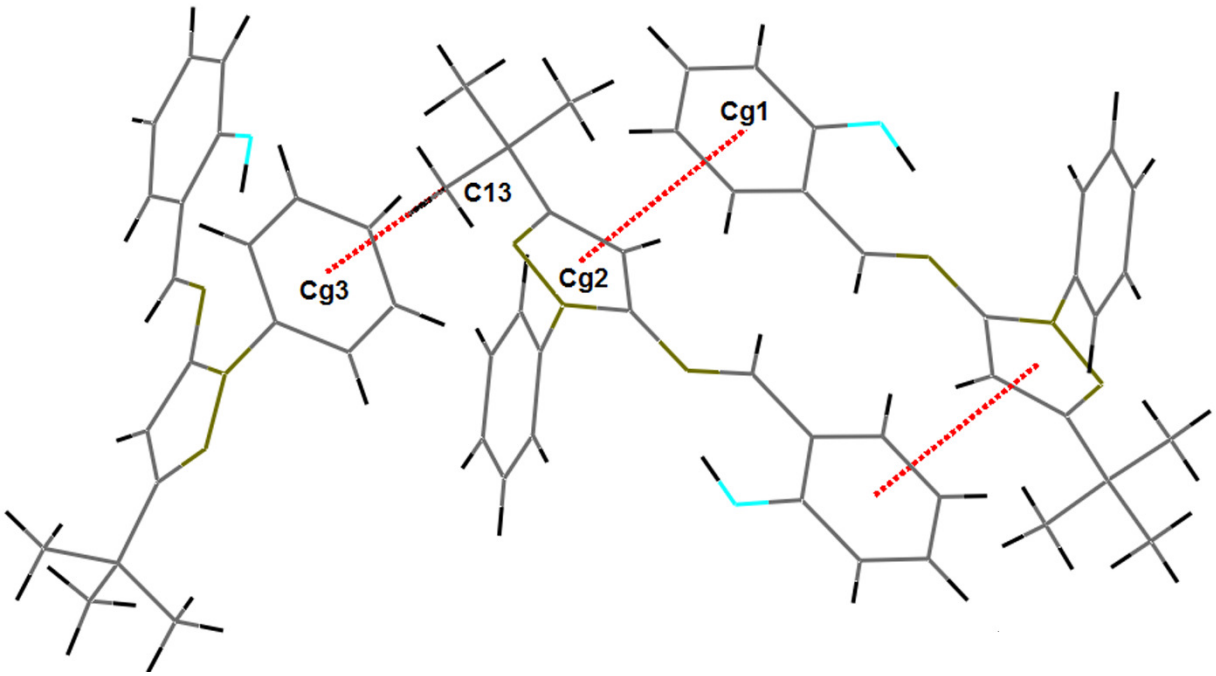

**(b)**

**Figure 2.** (a) Packing diagram of the title molecule parallel to (100). Dotted lines represent π…π and C-H…π interactions. (b) Interactions between $Cg_1$…$Cg_2$ and C-H…. $Cg_3$.

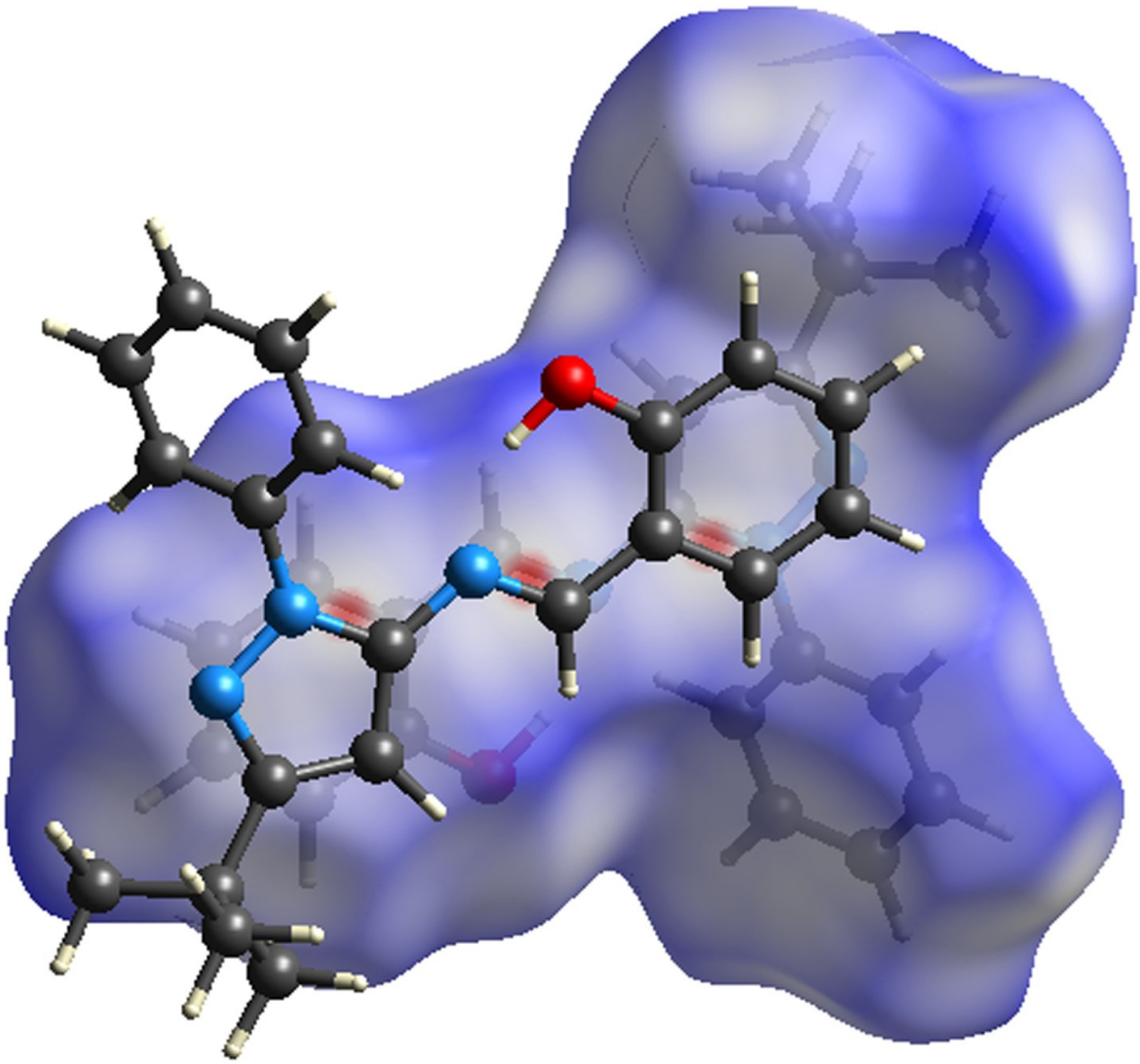

**(a)**

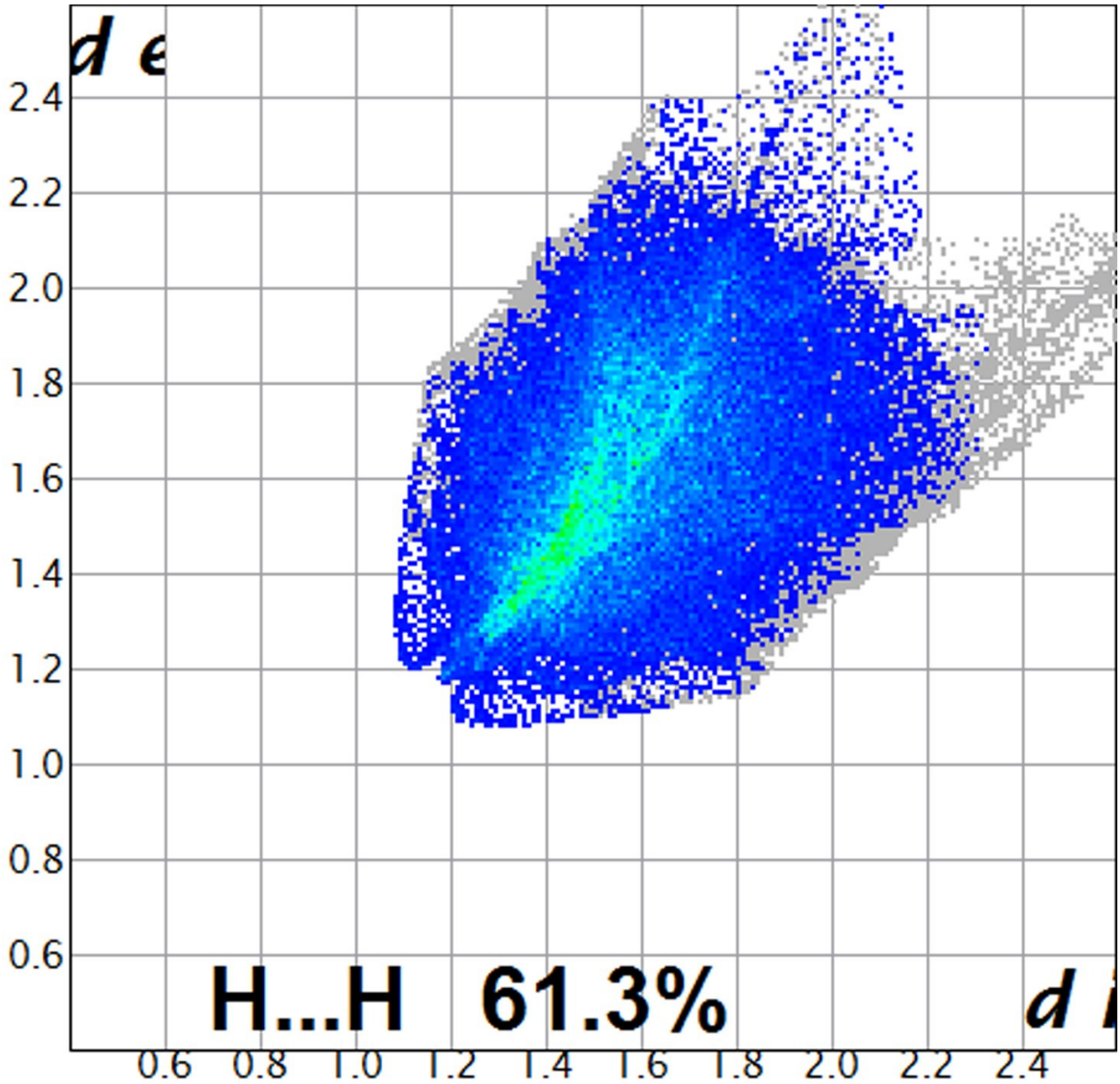


**(b)**

**Figure 3**. (a) ***dnorm*** mapped on Hirshfeld surface for visualizing the intercontacts. (b) Fingerprint H…H. ***di*** is the closest internal distance from a given point on the Hirshfeld surface and ***de*** is the closest external contacts.

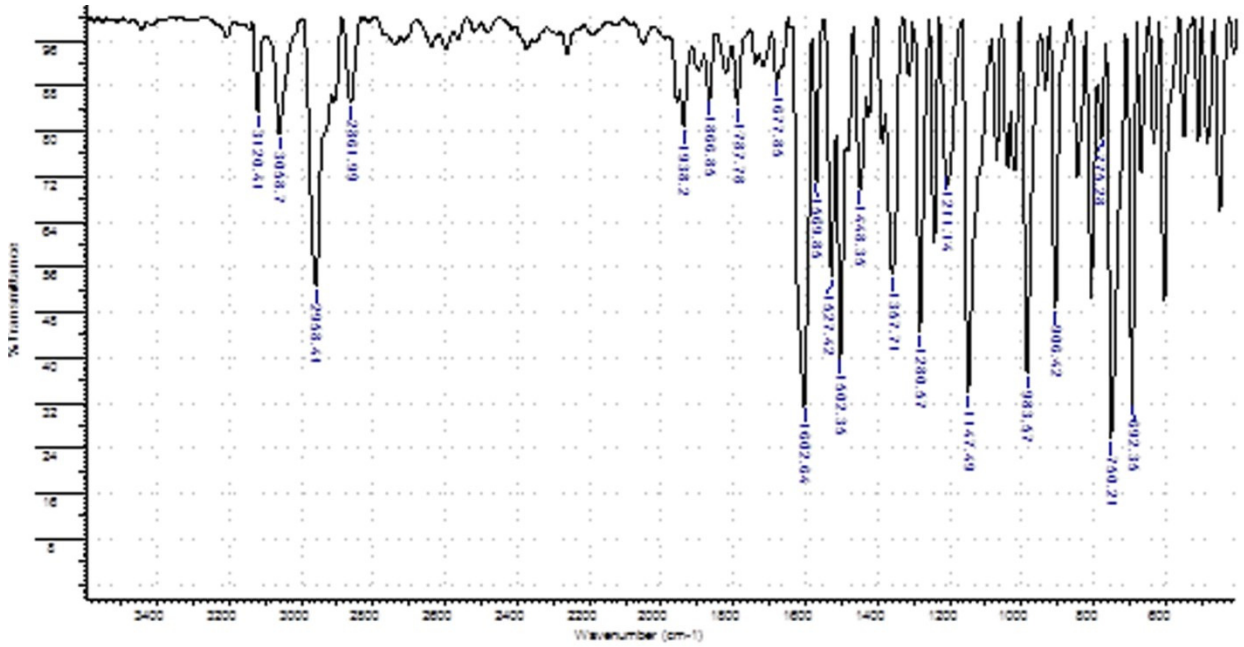


(a)

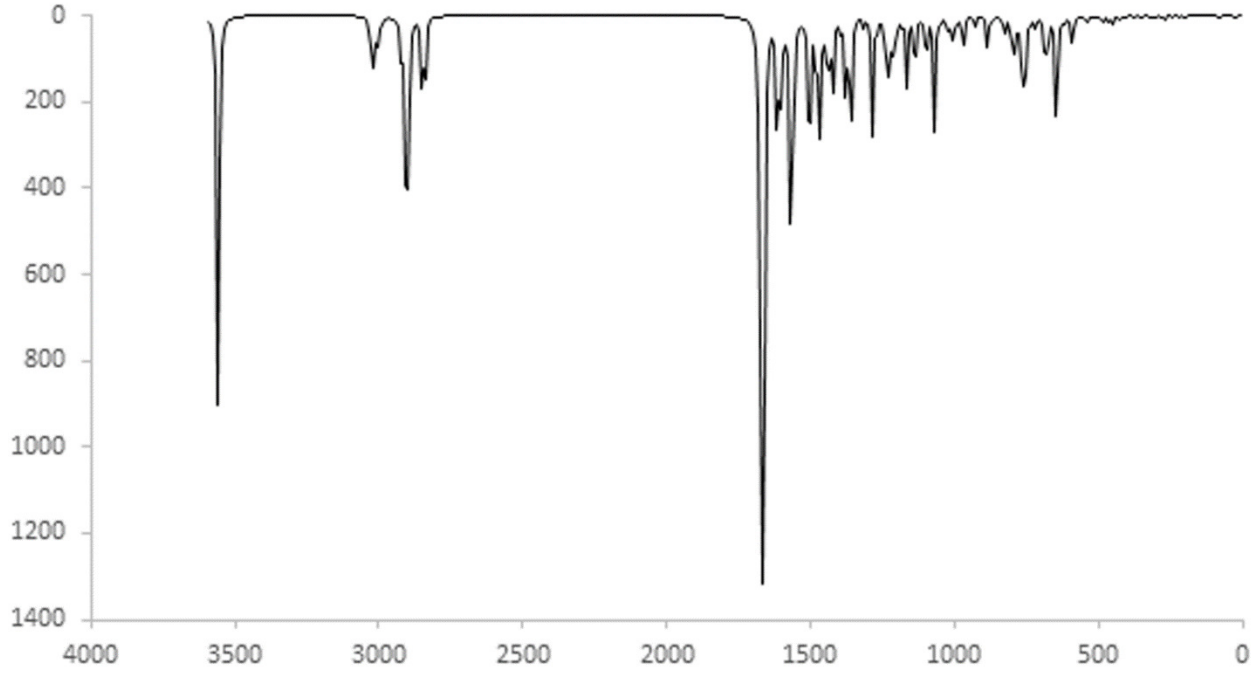


**(b)**

**Figure 4.** (a) Experimental FT-IR spectrum of compound **3**. (b) Theoretical IR spectrum of compound **3**.

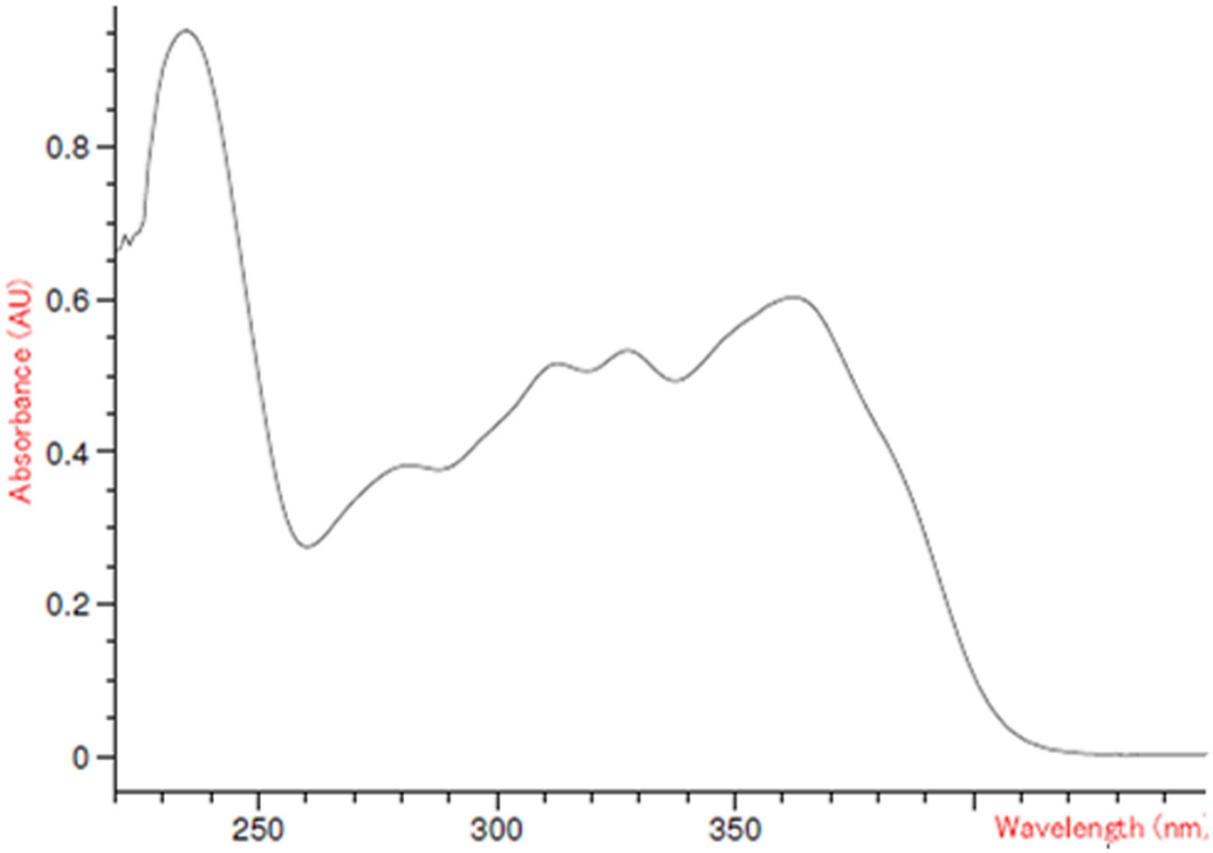


**(a)**

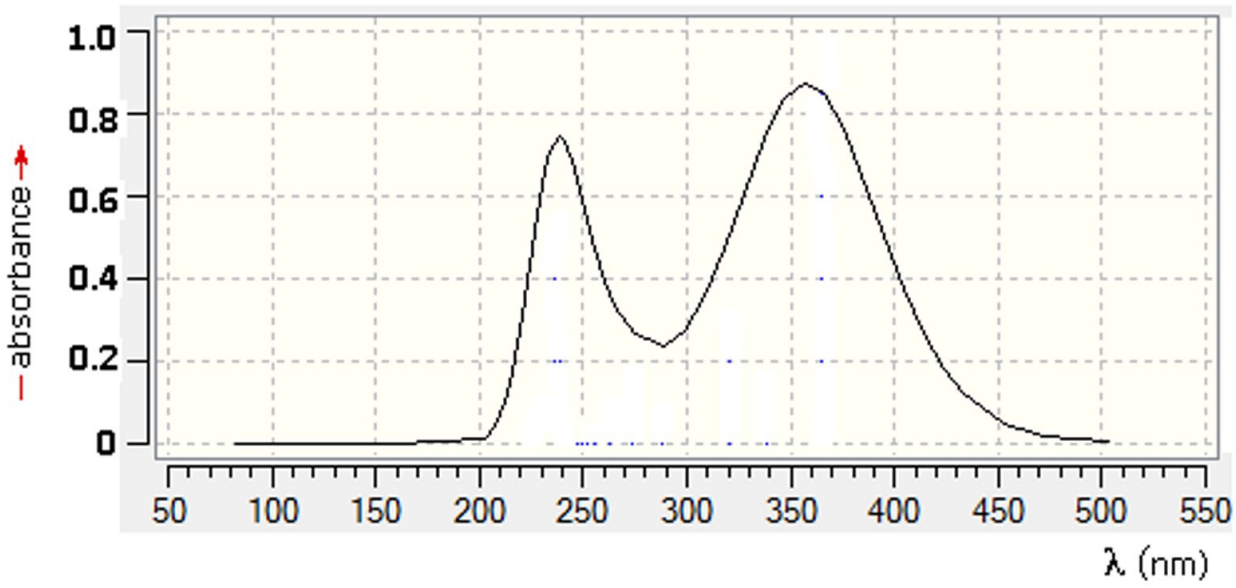


**(b)**

**Figure 5.** (a) Experimental ($CH_3CN$ solvent) and (b) calculated UV-Vis spectra of compound **3**.

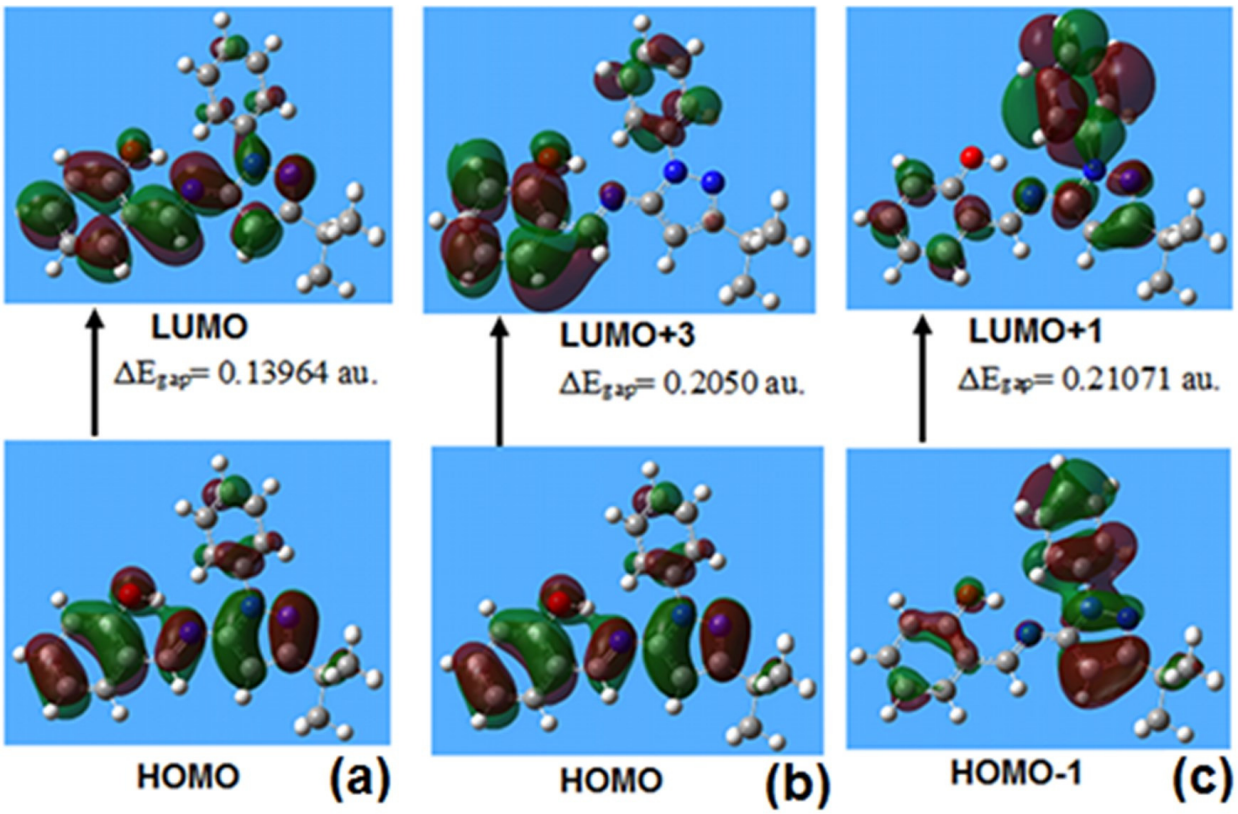


**Figure 6.** The HOMOs and LUMOs surfaces and energy values for compound **3**.